Supplemental Material: Effect of Boundary Scattering on Magneto-Transport Performance in BN-Encapsulated Graphene

Lijun Zhu(朱丽君)[1,2,3], Lin Li(李林)[1,2,3**], Xiaodong Fan(范晓东)[1,2,3],
Zhongniu Xie(谢忠纽)[1,2,3], and Changgan Zeng(曾长淦)[1,2,3**]

[1] CAS Key Laboratory of Strongly Coupled Quantum Matter Physics, and Department of Physics, University of Science and Technology of China, Hefei 230026, China

[2] International Center for Quantum Design of Functional Materials (ICQD), Hefei National Research Center for Physical Sciences at the Microscale, University of Science and Technology of China, Hefei 230026, China

[3] Hefei National Laboratory, University of Science and Technology of China, Hefei 230088, China

I. Fitting the low-field MR data for the SLG/SiO_2 device

The low-field MR data for the SLG/SiO_2 device were fit using the following formula that is widely used to describe the WL effect in graphene,[1,2]

$$\Delta\rho(\mathrm{B}) = -\frac{e^2\rho^2}{\pi h}\left[F\left(\frac{B}{B_\Phi}\right) - F\left(\frac{B}{B_\Phi + 2B_\mathrm{i}}\right) - 2F\left(\frac{B}{B_\Phi + B_\mathrm{i} + B_*}\right)\right]$$

where $F(z) = \ln z + \Psi(\frac{1}{2} + \frac{1}{z})$, $\Psi(x)$ is the digamma function, and $B_{\Phi,i,*} = \frac{\hbar}{4e}L_{\Phi,i,*}^{-2}$. L_Φ is the phase coherence length, and L_i/L_* is the inter/intra-valley scattering length. As demonstrated in Fig. 2b, the fitting is pretty good, and the typical lengths of L_Φ, L_i and L_* can be extracted accordingly.

II. Further analysis of bulk mean free path

The carrier density dependence of conductivity helps us to identify the dominant scattering sources in the present BN/SLG/BN devices.[3] We now discuss the dependence of conductivity on V_{BG} (see Fig. S4a), considering two main types of scattering events: short-range scattering and long-range charged-impurity scattering.[4] To extract the corresponding mean free path, the conductivity (σ) at different V_{BG} is fit using a formula that includes both long- and short-range scattering, $\sigma^{-1} =$

$(ne\mu_1)^{-1} + \rho_s$, where n is the carrier density, e is the elementary charge, μ_1 is the density-independent mobility from long-range charged-impurity scattering, and ρ_s is the resistivity from short-range scattering.[4-7] Typical fitting result at 1.5 K is shown in Fig.S4a (dashed line), from which μ_1 and ρ_s are obtained. Accordingly, the mean free path for long-range charged-impurity scattering ($L_{\text{long}} = \hbar\sqrt{\pi n}\mu_1 e^{-1}$) and for short-rang scattering ($L_{\text{short}} = \hbar\sqrt{\pi n^{-1}}\rho_s^{-1}e^{-2}$) at different V_{BG} can be extracted,[8] as presented in Fig. S4b. The value of L_{long} (L_{short}) increases (decreases) when the graphene sample is tuned away from the Dirac point, consistent with previous results.[4] Figures S4c,d show three types of mean free paths (L_{mfp}, L_{long} and L_{short}) as functions of V_{BG} on the electron- and hole sides, respectively. It is clear that L_{long} is smaller than L_{short} across a wider range of V_{BG}, i.e., the scattering rate $\tau_{\text{long}}^{-1} > \tau_{\text{short}}^{-1}$, demonstrating that charged-impurity scattering is the dominant scattering source within the bulk region. When the carrier density increases, the carrier screening effect is enhanced, leading to decreased charged-impurity scattering.

Supplemental figures:

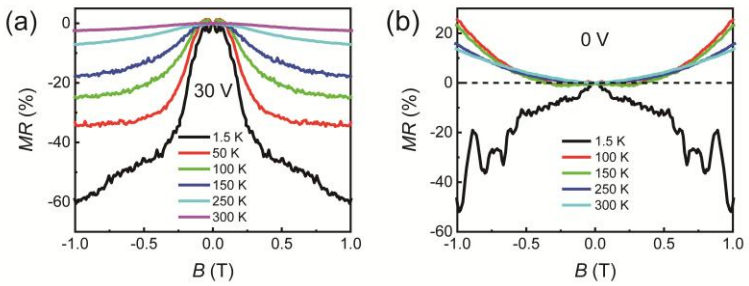

Fig. S1. MR curves measured at different temperatures for (a) V_{BG} = 30 V and (b) V_{BG} = 0 V. All data were obtained from the electron side.

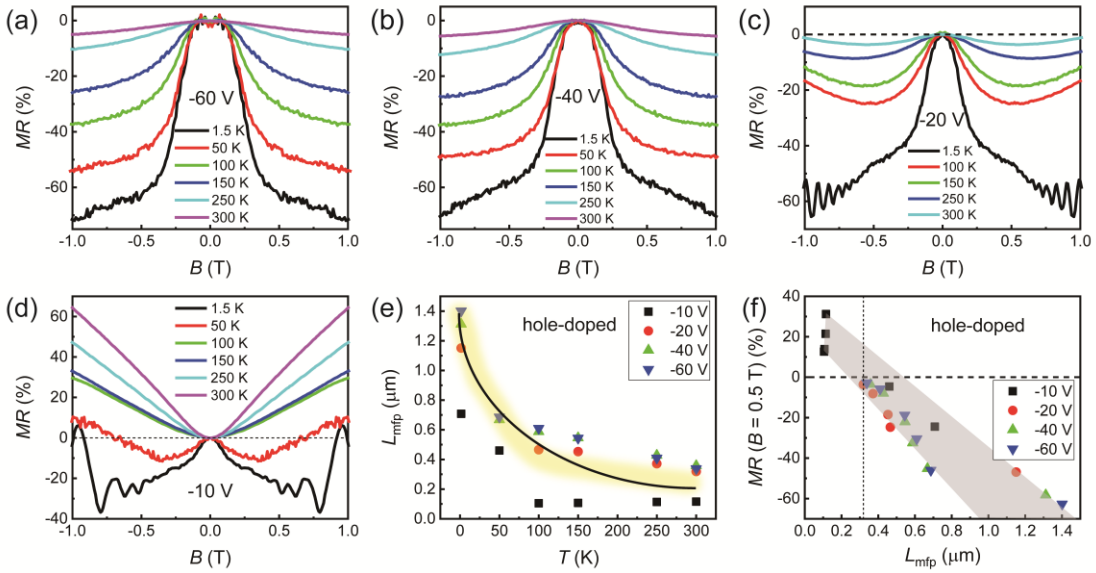

Fig. S2. Lower-limit of the bulk mean free path in the induction of boundary-scattering-dominated negative MR effect on the hole side. (a-d) MR curves measured at different temperatures for various V_{BG}: -60 V, -40 V, -20 V, -10 V. (e) Extracted values of L_{mfp} under different V_{BG} as a function of temperature. The black line serves as a guide to the eyes. (f) Relationship between the MR value at B = 0.5 T and the L_{mfp}. Corresponding data were obtained on the hole side over a range of V_{BG} and temperature. Here, the lower-limit of the ballistic ratio is 0.16 (i.e. L_{mfp}/W = 0.32 μm/2 μm), which is similar to the result obtained from the electron side (see Fig. 3d in the main text).

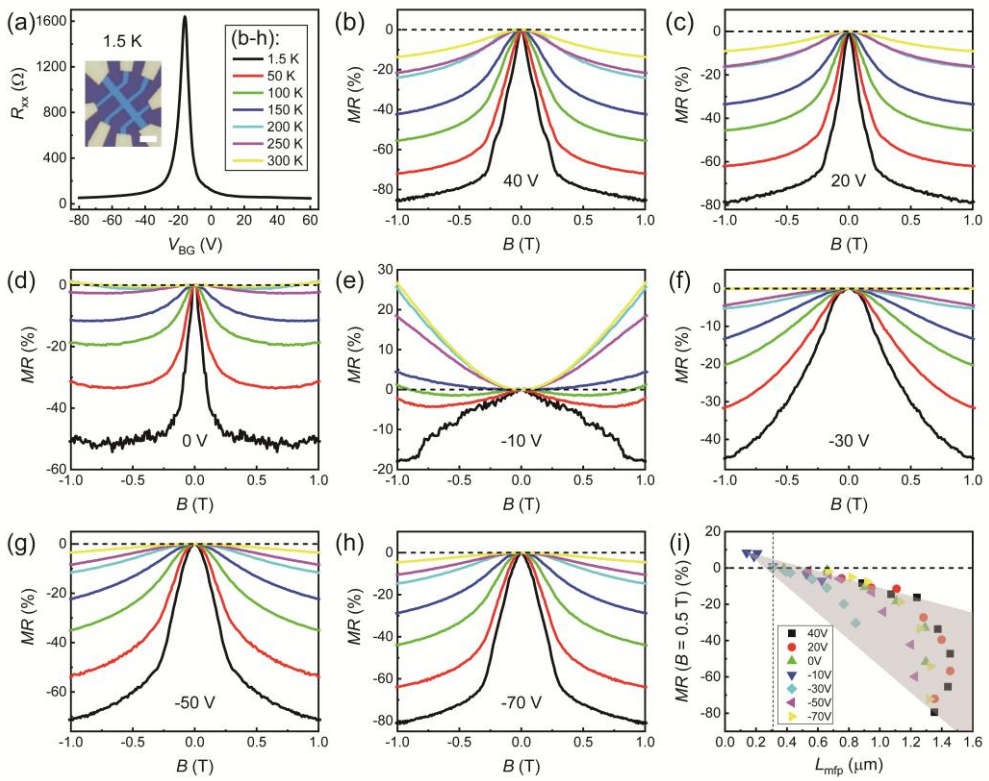

Fig. S3. Magneto-transport behaviors of a BN-encapsulated bilayer graphene device. (a) R_{xx} as a function of V_{BG} measured at 1.5 K. Inset: optical microscope image of the device. (b-h) MR curves obtained at different temperatures for various V_{BG}. (i) Relation between the MR value at B = 0.5 T and the extracted L_{mfp}. The black dashed line indicates the lower-limit of L_{mfp} for inducing boundary-scattering-dominated negative MR effect.

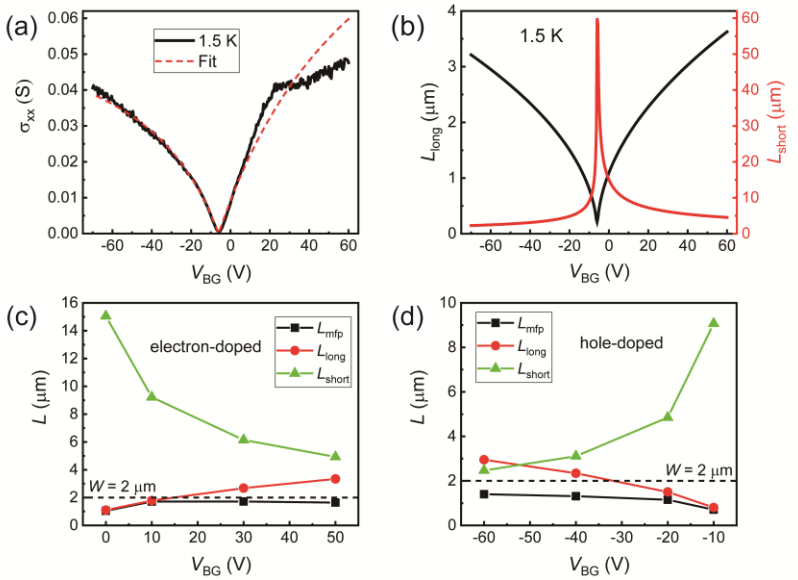

Fig. S4. Extracting L_{long} and L_{short} at different V_{BG}. (a) Conductivity (σ) as a function of V_{BG} at 1.5 K. The dashed line is fitted by the formula presented in supplementary Note 2. (b) The obtained L_{long} (black line) and L_{short} (red line) as functions of V_{BG}. (c,d) L_{mfp}, L_{long}, and L_{short} as functions of V_{BG} on the electron and hole sides, respectively.

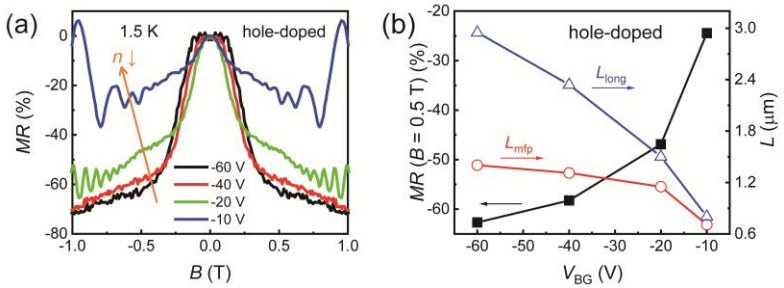

Fig. S5. Evolution of the MR effect with varying V_{BG} on the hole side. (a) MR curves for different V_{BG} measured at 1.5 K. (b) MR value at B = 0.5 T (black line) and extracted values of L_{mfp} (red line) and L_{long} (blue line) as functions of V_{BG} at 1.5 K. The corresponding values of carrier density at each value of V_{BG} can be found in Fig. 1c. It is clear that the amplitude of negative MR increases monotonically with increasing L_{long} at different V_{BG}, consistent with the results obtained from the electron side (see Fig. 4 in the main text).

Supplemental references:

[1] McCann E, Kechedzhi K, Fal'ko V I, Suzuura H, Ando T and Altshuler B L 2006 *Phys. Rev. Lett.* **97** 146805

[2] Wu X, Li X, Song Z, Berger C and de Heer W A 2007 *Phys. Rev. Lett.* **98** 136801

[3] Peres N M R 2010 *Rev. Mod. Phys.* **82** 2673

[4] Masubuchi S, Iguchi K, Yamaguchi T, Onuki M, Arai M, Watanabe K, Taniguchi T, and Machida T 2012 *Phys. Rev. Lett.* **109** 036601

[5] Nomura K and MacDonald A H 2007 *Phys. Rev. Lett.* **98** 076602

[6] Hwang E S, Adam S and Sarma S D 2007 *Phys. Rev. Lett.* **98** 186806

[7] Dean C R, Young A F, Meric I, Lee C, Wang L, Sorgenfrei1 S, Watanabe K, Taniguchi T, Kim P, Shepard K L and Hone J 2010 *Nat. Nanotechnol.* **5** 722

[8] Sarma S D, Adam S, Hwang E H and Rossi E 2011 *Rev. Mod. Phys.* **83** 407